



Validation strategies of HIMAG in interfacial flow computation for fusion applications

Ming-Jiu Ni^{a,*}, Ramakanth Munipalli^b, Neil B. Morley^a, Mohamed A. Abdou^a

^a Department Mechanical and Aerospace Engineering, University of California at Los Angeles, 43-133 Engineering IV, CA 90095, USA

^b HyPerComp Inc., 31255 Cedar Valley Dr., Westlake Village, CA 91362-4014, USA

Received 5 February 2005; received in revised form 16 September 2005; accepted 16 September 2005

Available online 27 December 2005

HIMAG, a 3-D incompressible MHD free surface code developed by HyPerComp Inc., in a joint research project with UCLA has been successfully applied for APEX [M.A. Abdou, A. Ying, N. Morley, et al., On the exploration of innovative concepts for fusion chamber technology, APEX Interim Report Overview, Fusion Eng. Des. 54 (2001) 181–247] and fusion relevant cases [R. Munipalli, V. Shankar, M.-J. Ni, N. Morley, et al., Development of a 3-D incompressible free surface MHD computational environment for arbitrary geometries: HIMAG DOE phase-II SBIR, period of performance: June 2001–June 2003, Final Report, June 2003; N. Morley, S. Smolentsev, N. Munipalli, M.-J. Ni, D. Gao, M. Abdou, Progress on the modeling of liquid metal, free surface, MHD flows for fusion liquid walls, Fusion Eng. Des. 72 (2004) 3–34] including LIMITS and NSTX. This unique code was developed to model multiple solid and liquid phase materials with arbitrary geometry. The inclusion of complex-geometry, electrically conducting walls and nozzles are essential since electric current closure paths are typically through these solid structures. In HIMAG, a second-order variable density projection method is used to simulate incompressible Navier–Stokes equations and the level set method is used to capture free surfaces. HIMAG is developed on unstructured grids, and can be run in parallel across multiple processors, and is thus able to efficiently solve large complex problems. HIMAG has already been validated for steady and unsteady single-fluid flow with/without MHD effects. In this paper, we demonstrate some validation cases for interfacial flows using HIMAG.

© 2005 Elsevier B.V. All rights reserved.

Keywords: Computational methods; MHD; Free surface; Level set; Validation

1. Introduction

The motion of incompressible fluid with free surfaces in the presence of a magnetic field represents a

unique and intriguing blend of issues in fluid physics and electromagnetics. Fig. 1 shows the complex synergy of physical phenomena present in such a flow when applied to a heat extraction concept in nuclear fusion. Motivation for this code development comes from concerns in the nuclear fusion community on the modeling of liquid metal walls in fusion reactors [1]. Apart from being a useful means of extracting heat from

* Corresponding author. Tel.: +1 310 794 9198; fax: +1 310 825 2599.

E-mail address: mingjiu@fusion.ucla.edu (M.-J. Ni).

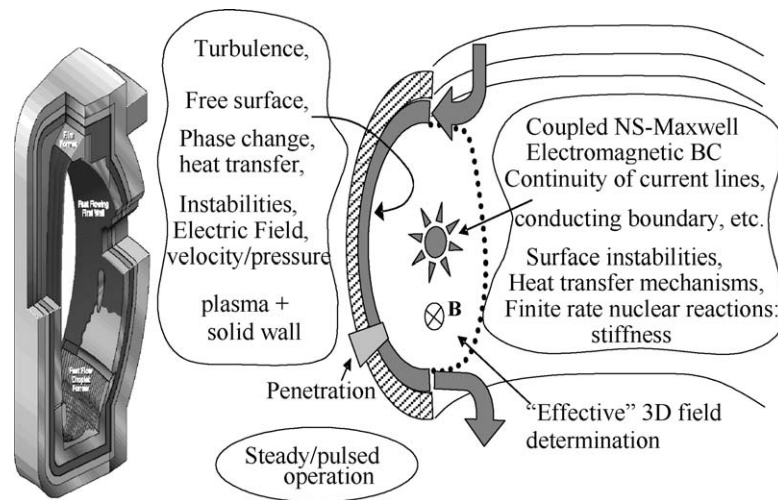


Fig. 1. A section of a tokamak design with liquid walls (left) and a description of its multi-physical nature.

the intense plasma core of the reactor and protect structural components from continuous exposure to radiation, liquid lithium (one of the candidate fluids for this purpose) produces tritium when exposed to the neutron radiation, which may be regeneratively used in the reactor as fuel. There are strong commercial applications of incompressible flows with MHD. These include the electromagnetic stirring of metals, contact-less processing of aluminum and steel and the use of liquid metal walls in nuclear fusion reactors for heat absorption, all of which are very active areas of research in the present time. HyPerComp Inc., in collaboration with the Fusion Engineering group at the University of California at Los Angeles has developed a high fidelity simulation tool named HyPerComp Incompressible MHD solver for Arbitrary Geometries (HIMAG) which is a time-accurate magneto-hydrodynamics (MHD) solver for three-dimensional multiphase flows on unstructured or hybrid meshes. Apart from this unique blend of multi-physical phenomena in fluid media, HIMAG is able to also compute electromagnetic and thermal quantities in solid walls using a variety of methods. Graphical user interfaces accompany the code, to set up boundary conditions, and to partition the mesh system such that the problem may be solved across multiple processors.

In the present form of HIMAG, the following capabilities are available: (1) three-dimensional incompressible flow solver (second-order accurate in space and time); (2) free surface capture using level set

technique; (3) arbitrary mesh structure (unstructured/hybrid); (4) parallel code environment; (5) computation of electromagnetic fields using the electric potential; (6) point implicit scheme, solved in an iterative manner; (7) multiple strategies to account for mesh skewness (non-orthogonality); (8) modular addition of source terms; (9) graphical user interfaces.

This solver has been validated using steady and unsteady canonical problems based on comparable analytical and numerical data. Insulating wall MHD in 2-D and 3-D steady and unsteady problems has been demonstrated. By use of appropriate meshes it has been possible to run cases at fairly large Hartmann numbers [2,3]. In this paper, we demonstrate the validation of HIMAG for multi-phase flows with significant interfacial deformation.

2. Validation of HIMAG for interfacial flows

There has been interest in simulating two-fluid flows where the density of the first fluid is considerably higher than the second. Such flows are found abundantly in nature, and also dominate several critical industrial processes. Since the primary fluid in most of these situations is virtually incompressible (water, liquid metal, etc.) the set of incompressible Navier–Stokes equations is used to model them. The validation of HIMAG for interfacial flows has been conducted, which include the validation of surface tension; mass conservation of a

level set method; temporal accuracy of interface evolving. 3-D bubble rising in a channel is also conducted on multi-processors.

2.1. Surface tension model test

A rigorous validation of the surface tension terms in HIMAG has been undertaken. A sample problem, one of a square droplet at a Weber number of 10 has been considered. The droplet, must ideally deform until a circular shape is attained. At this point, the pressure difference between inside and outside the droplet can be matched with the analytical value given by the surface tension force. Also, from mass conservation considerations, the diameter of the circular droplet can be determined exactly. These have been seen to be satisfied well by HIMAG. A further interesting effect has been noticed, that the droplet performs oscillations before settling down to a circular shape, and these oscillations depend upon the viscosity in the fluid that resists motion. Two series of images are shown below, corresponding to (Fig. 2(a)) a high viscosity case, in which

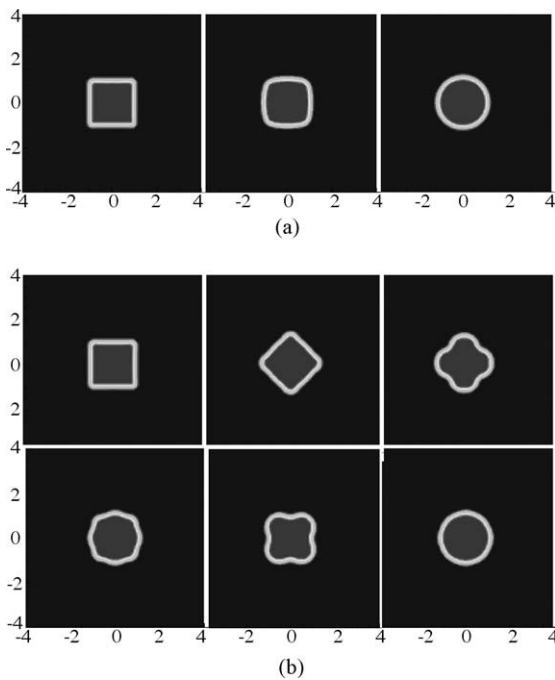


Fig. 2. Bubble motion driven by surface tension: (a) high viscosity and (b) low viscosity.

circular shape is attained without many oscillations; (Fig. 2(b)) a low viscosity case, in which several mode shapes are observed and oscillations persist for much longer.

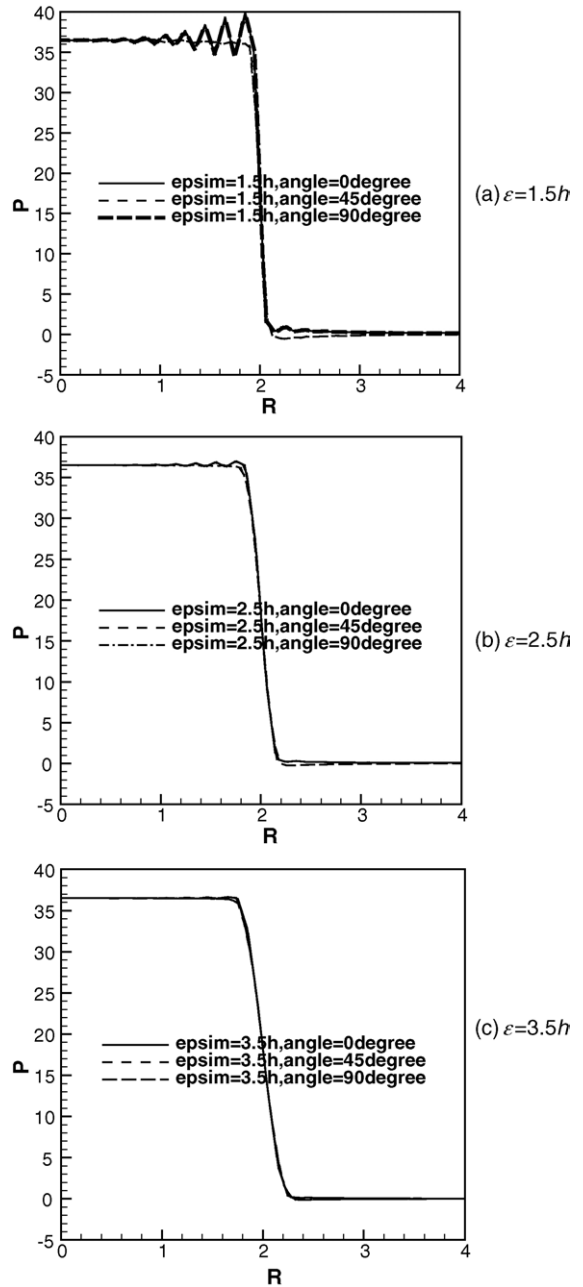


Fig. 3. Pressure profiles using HIMAG along radial direction at angles 0°, 45°, 90°.

Table 1
Error in pressure and velocity with the CSF model using HIMAG

| R/h | Δt | Time step | $ [P]_{\text{drop}} - [P]_{\text{theory}} $ | $ u _{\text{max}}$ |
|-------|------------|-----------|---|-----------------------|
| 5 | 10^{-4} | 10 | 0.40376 | 2.64×10^{-3} |
| 5 | 10^{-5} | 100 | 0.40089 | 2.32×10^{-3} |
| 10 | 10^{-4} | 10 | 6.94×10^{-2} | 4.91×10^{-3} |
| 10 | 10^{-5} | 100 | 6.86×10^{-2} | 5.11×10^{-3} |
| 20 | 10^{-4} | 10 | 1.32×10^{-2} | 1.11×10^{-2} |
| 20 | 10^{-5} | 100 | 1.10×10^{-2} | 1.03×10^{-2} |

A good quantitative check for the validity the level set method [4] and CSF model [5] for the surface tension term employed in HIMAG is to consider a circular droplet in the absence of gravity and viscous effects. The exact jump in pressure across the droplet is then given by: Laplace’s formula as:

$$[P]_{\text{theory}} = P_{\text{drop}} - P_{\text{back}} = \frac{k}{We} \quad (1)$$

here We denotes Weber number defined in Section 2.4. The exact curvature for this case is $k = 1/R$. For the test, we choose $We = 1.73$, computational domain $\Omega = [0,8] \times [0,8]$. The droplet is initially placed at the center of the domain, and has a radius $R = 1.0$. The density of droplet is $\rho_{\text{drop}} = 10$, and the density of the background fluid is $\rho_{\text{back}} = 1$. The exact pressure difference $[P] = 36.5$. The error in the pressure jump and in the maximum velocity is investigated. The numerical jump in pressure is evaluated as $[P_{\text{drop}}] = P_{\text{in}} - P_{\text{out}}$, where the subscript “in” denotes inside the drop (averaged in $r < R/2$) and “out” outside the drop (averaged

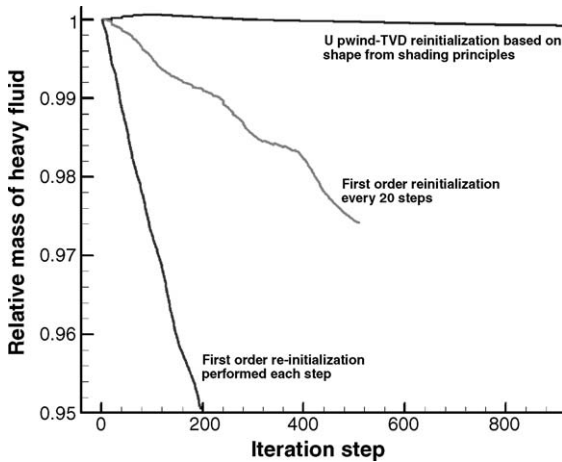


Fig. 4. Mass conservation errors in the level set implementation.

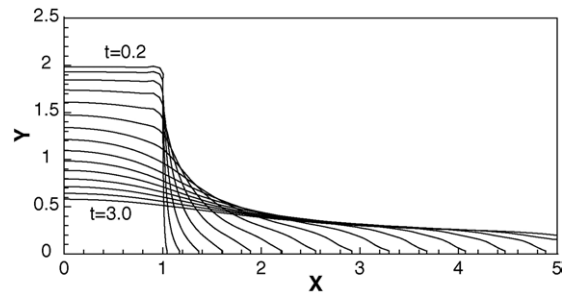


Fig. 5. Zero level set contour from time = 0.2 to 3.0 with time interval 0.2.

in $r > 3R/2$). Here R , ρ_{drop} , ρ_{back} and $[P]$ are all normalized as dimensionless parameters with $R = 1.0$ and $\rho_{\text{back}} = 1$.

First, we check the effect of ε (ε is a small positive number for the smoothness of density and viscosity across the interface) on the CSF tension model. A uniform grid with $R/h = 20$ (h is a grid cell length) is used. The test case is calculated using HIMAG with $\varepsilon = 1.5h$,

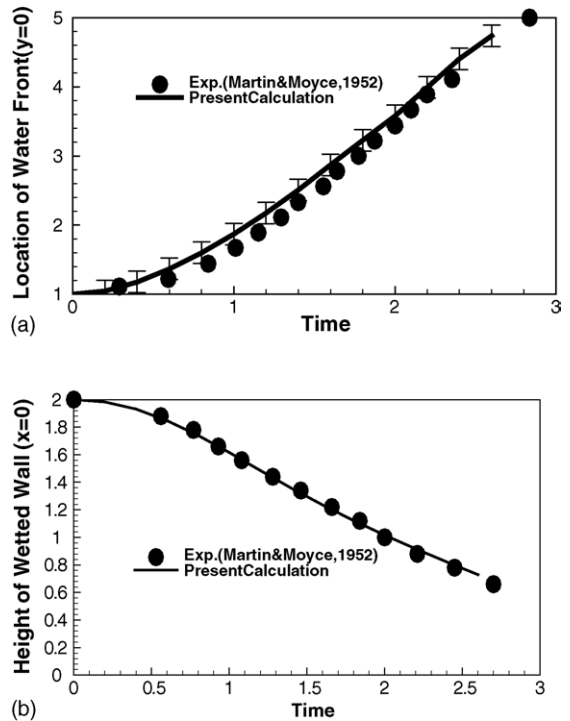


Fig. 6. History of water front location on solid surfaces in the dam break: (a) location of water front at $y = 0$; (b) height of wetted wall at $x = 0$.

2.5*h* and 3.5*h*, respectively. Fig. 3 shows the computed pressure profiles with CSF model along radial direction at angles 0°, 45° and 90°. From this figure, we can see a strong oscillation of pressure across the interface for the case of $\epsilon = 1.5h$, the oscillation is greatly reduced for the case of $\epsilon = 2.5h$ and finally the oscillation is disappear for the case of $\epsilon = 3.5h$.

Having known the performance of CSF model and the effect of ϵ on the model, now we study the performance of the projection method employed in HIMAG by running the test. The results at $t = 0.001$ are shown in Table 1. Here t is a dimensionless parameter.

In all of the calculations, the curvature rate is calculated based on a smooth level set function. From this table, we can see that calculation of surface tension

using HIMAG is pretty accurate comparing with the theoretical solution.

2.2. Mass conservation of the level set method employed in HIMAG

The level set method has often faced criticisms concerning the conservation of mass. We have developed a higher order accurate mass conserving upwind based level set technique, based on a shape from shading approach of Ruoy–Tourin [6]. The oscillating square droplet described earlier was used in estimating mass loss errors. The ratio of the mass of heavy fluid at a given time to the initial mass at the onset of computation is plotted in Fig. 4. In HIMAG, we have found this

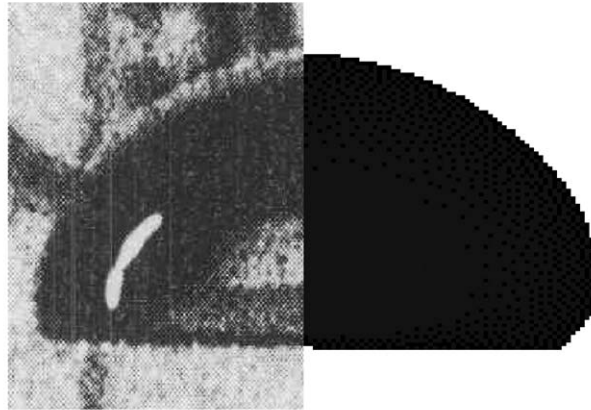


Figure 3e of Bhaga & Weber, $E\ddot{o}=116$; $M=1.31$ Present $E\ddot{o}=116$; $M=1.31$

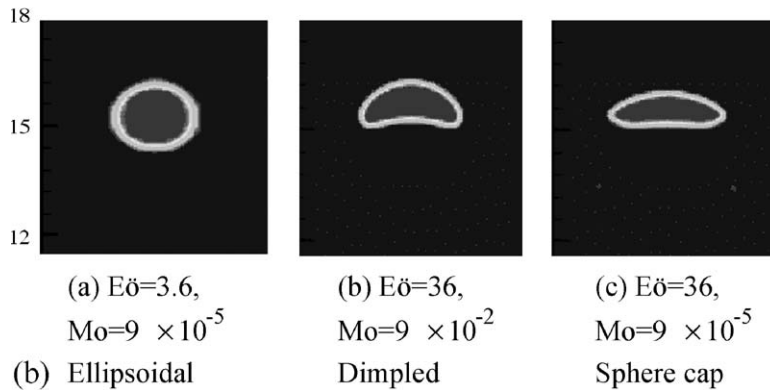


Fig. 7. Shapes compared with numerical and experimental results: (a) shapes compared with Bhaga and Weber’s; (b) shapes consistent with Grace General Formula.

method of TVD procedure [7] together with an arbitrary mesh version of the shape-from-shading method is very accurate, and preserves mass to 0.04% accuracy as compared to the 10–15% errors observed in the other methods.

2.3. Temporal accuracy of HIMAG for interfacial flows: dam break

The broken dam of Martin and Moyce [8] problem is calculated to further validate the methods employed in HIMAG by comparing the numerical result with the experimental data. A 81×41 uniform Cartesian grid is used with initial water column height to width ratio of 2. $\rho_{\text{water}}/\rho_{\text{back}} = 1000$, $\mu_{\text{water}}/\mu_{\text{back}} = 1000$ and $Re = 1000$. At the outlet boundary, the Neumann boundary condition is used for velocities. At all other boundaries, slip wall boundary conditions are applied. Fig. 5 illustrates the free surface profiles between time = 0.2 and 3.0 with time interval 0.2. The water surface evolves in smooth shape and no oscillation occurs at the interface near the solid wall. Fig. 6(a) shows the history of water front marching along the ground surface ($y = 0$) and Fig. 6(b) shows the transient height of wetted wall along the vertical surface ($x = 0$). Also the error bar in Fig. 6 shows the interface height in this calculation. The experiment results from Martin and Moyce [8] are also shown in Fig. 6. The numerical results match the experimental data well. All parameters shown in Figs. 5 and 6 are normalized as defined by Martin and Moyce [8].

2.4. Bubble rising in a channel

The study of droplet deformation and breakup is of great importance in many applications such as mixing in multiphase systems, blending of molten polymers, ink-jet printers, deformation of biological cells, drawing of glass sheets and others. Now we use HIMAG to simulate bubble rising in a channel. An initially stationary sphere bubble of diameter $2R_0$ is released from a position near the bottom wall in a rectangular channel with the length and width $6R_0$ and depth $18R_0$. The bubble is lighter than the fluid and starts to move up driven by buoyancy. Defining the characteristic velocity and length as $U = (gR_0)^{1/2}$ and $L = R_0$, respectively, we have dimensionless groups of Reynolds, Froude and Weber numbers as $Re = \rho_1 g^{1/2} R_0^{3/2} / \mu_1$, $Fr = 1$ and $We = \rho_1 g R_0^2 / \sigma$, Morton number $Mo =$

$(g\mu_L^4(\rho_L - \rho_G)/\rho_L^2\sigma^3)$ and Eötvös number $E\ddot{o} = g(\rho_L - \rho_G)d_0^2/\sigma$. (The top boundary is set as an open boundary condition; all other boundaries are non-slip wall conditions.)

With a grid of $60 \times 60 \times 180$ employed, we simulate the case of $Mo = 1.31$ and $E\ddot{o} = 161$, Fig. 7(a) shows that our computational interface shape is very consistent the experimental result from Bhaga and Weber [9]. Fig. 7(b) further shows that our computational shapes are very consistent with Grace's graphical correlation [10] in a big region of Mo (from $Mo = 9 \times 10^{-2}$ to 9×10^{-5}) and $E\ddot{o}$ (from $E\ddot{o} = 3.6$ to 36) numbers. Also the inner circulation is shown in our computational result.

The shapes development of a bubble rising up in a liquid with a density ratio of 10, viscosity ratio of 10, Reynolds number of 10 are shown in Fig. 8(a) for the case of Weber number 1 and shown in Fig. 8(b) for the case of Weber number 10, respectively. The deformation and velocity of bubble rising up in a channel can be seen. The effect of surface tension can be illustrated in these two figures. We are applying HIMAG for the further investigation effects of inertial, viscous force, surface tension on the bubble rising up in a channel, and are making comparison with the results from [11].

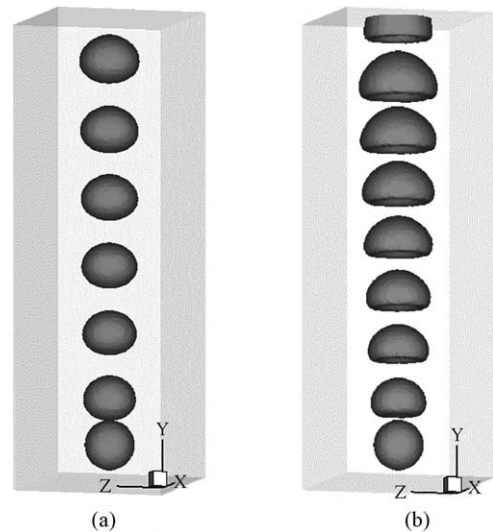


Fig. 8. Bubble rising in a channel by HIMAG: (a) $Re = 10$; $We = 1$; density ratio = 10; viscosity ratio = 1; time from 0 to 18 with interval 3; (b) $Re = 10$; $We = 1$; density ratio = 10; viscosity ratio = 1; time from 0 to 24 with interval 3.

3. Conclusion

Validation cases of HIMAG for interfacial flows have been presented. We use HIMAG to simulate surface driven flows, dam broken case and bubble rising driven by gravity force. The numerical results show that HIMAG has good accuracy and mass conservation for the simulation of multi-fluid flows with large deformation. The applications of HIMAG for interfacial MHD, such as LIMITS and NSTX have been conducted, and the simulation result of NSTX is shown in a different paper at this conference. These validations have been run on both single PC and parallel cluster computers.

Acknowledgments

This work is supported by the U.S. Department of Energy under Grant #DE-FG03-86ER52123 and DOE SBIR Grant #DE-FG02-04ER83977.

References

- [1] M.A. Abdou, The APEX Team, On the exploration of innovative concepts for fusion chamber technology, APEX interim report overview, *Fusion Eng. Des.* 54 (2001) 181–247.
- [2] R. Munipalli, V. Shankar, M.-J. Ni, N. Morley, Development of a 3-D incompressible free surface MHD computational environment for arbitrary geometries: HIMAG DOE phase-II SBIR, period of performance: June 2001–June 2003, Final Report, June 2003.
- [3] N. Morley, S. Smolentsev, N. Munipalli, M.-J. Ni, D. Gao, M. Abdou, Progress on the modeling of liquid metal, free surface, MHD flows for fusion liquid walls, *Fusion Eng. Des.* 72 (2004) 3–34.
- [4] S. Osher, J.A. Sethian, Fronts propagating with curvature-dependent speed, algorithms based on Hamilton–Jacobi formulation, *J. Comput. Phys.* 79 (1988) 12–49.
- [5] J.U. Brackbill, D.B. Kothe, C. Zemach, A continuum method for modeling surface tension, *J. Comput. Phys.* 100 (1992) 335–354.
- [6] E. Ruoy, A. Tourin, A viscosity solutions approach to shape from shading, *SIAM J. Numer. Anal.* 29 (1992) 867–884.
- [7] T.J. Barth, Aspects of unstructured grids and finite volume solvers for the Euler and Navier–Stokes equations, *Von Karman Inst. Lect. Ser.* 1994–05 (1994) 1–141.
- [8] J.C. Martin, W.J. Moyce, An experimental study of the collapse of liquid columns on a rigid horizontal plane, *Philos. Trans. R. Soc. Lond. Ser. A Math. Phys. Sci.* 244 (1952) 312–324.
- [9] D. Bhaga, M.E. Weber, Bubbles in viscous liquids: shapes, wakes and velocities, *J. Fluid Mech.* 105 (1981) 61–85.
- [10] J.R. Grace, Shapes and velocities of bubbles rising in infinite liquids, *Trans. Inst. Chem. Eng.* 51 (1973) 116–120.
- [11] G. Ryskin, L.G. Leal, Numerical solution of free-boundary problems in fluid mechanics. Part I. The finite-difference technique, *J. Fluid Mech.* 148 (1984) 1–17.